# ANALYTICAL PREDICTION OF EDDY-CURRENT LOSSES IN FRACTIONAL SLOT PM MACHINES

Asma Masmoudi Ahmed Masmoudi
Research Unit on Renewable Energies and Electric Vehicles
University of Sfax, Sfax Engineering School, BP W, 3038 Sfax, Tunisia
E-mail: asma_masmoudi@yahoo.fr, a.masmoudi@enis.rnu.tn

***Abstract:*** *Fractional slot permanent magnet machines are gaining interest in propulsion applications. However, they are penalized by the production of flux densities waveforms with dense harmonic contents, leading to additional losses in the magnets as well as in the back iron compared to distributed winding machines. In this paper, an analytical prediction of eddy-current losses in the back iron including rotor and stator yokes is provided considering a 10pole/12slot double-layer machine. The influence of skin depth is taken into consideration for the high harmonic frequencies. It has been found that considering just eddy-currents caused by the synchronous harmonic leads to very underestimated losses.*

***Key words:*** *permanent magnet machines, concentrated winding, distributed winding, eddy-current losses, harmonic content, skin effect.*

## 1. INTRODUCTION

FRACTIONAL slot permanent magnet machines (FSPMM) are drawing more and more attention in propulsion systems as far as they exhibit high power and torque densities. Furthermore, they exhibit low cogging torque, wide flux weakening range, and interesting fault-tolerance capabilities [1], [2]. However, concentrated windings generate M.M.F with denser harmonic contents than the ones of optimally designed distributed windings. These harmonics moving asynchronously with the rotor, lead to an inevitable increase of eddy-current losses in the magnetic circuit.

The paper deals with an analytical approach to predict the eddy-current losses in the core of a 10pole/12slot PM machine. Such a topology has been widely considered in the literature [1], [2], [3], [4].

It has been reported that several teams have been involved in the calculation of iron losses in conventional machines [5], [6]. The proposed models were generally limited to the contribution of the synchronous harmonic in the iron losses.

However, relatively few published material dealing with iron loss assessment in FSPMM has been reported in the literature. *Polinder* et al. [7] treated the calculation of eddy-current of solid rotor back iron of fractional slot linear PM machine. In [8], *Bianchi* et al. adopted a straight-lined 2-D analytical model for the calculation of the eddy-current losses in a solid rotor CWPMM.

The contribution of this paper consists in an analytical prediction of the eddy-current losses in the stator yoke lamination as well as in the rotor one, accounting for the skin effect.

## 2. PROBLEM FORMULATION

Eddy-currents are induced in ferromagnetic core when a ferromagnetic circuit is exposed to a temporal variation of a flux density field. The direction of those currents is given by Lenz's law as illustrated in figure 1.

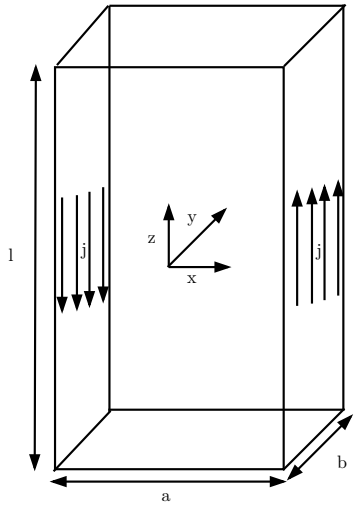


Fig. 1. Eddy-current induction in laminated magnetic circuit

Then the total eddy-current loss in a lamination sheet may be expressed as [9]:

$$P_e = \frac{\omega^2 \hat{\phi}^2 \sigma b \delta}{8l} \left( \frac{\sinh(a/\delta) - \sin(a/\delta)}{\cosh(a/\delta) - \cos(a/\delta)} \right) \qquad (1)$$

where:

- $\sigma$ is the conductivity of the material,
- $a$ is the lamination sheet thickness,
- $\omega$ is the considered velocity,
- $\hat{\phi}$ is the maximum value of the total magnetic flux,
- $\delta = \sqrt{\frac{2}{\omega\mu\sigma}}$ is skin depth or depth penetration, where $\mu = \mu_0\mu_{rfe}$, is the magnetic permeability of the lamination.

From the previous formulation, two cases could be distinguished:

- at low frequency, ie, when $\frac{a}{\delta} \ll 1$, the total eddy current losses in a lamination sheet is expressed as:

$$P_{el} = \frac{\omega^2\hat{\phi}^2\sigma ba}{24l} \tag{2}$$

- at high frequency when skin effect predominates, ie, when $\frac{a}{\delta} \gg 1$, the total eddy current losses in a lamination sheet is expressed as:

$$P_{eh} = \frac{\omega^2\hat{\phi}^2\sigma b\delta}{8l} \tag{3}$$

The variations of the skin depth $\delta$ to sheet length $a$ ratio in rotor and stator laminations are illustrated in figures 2 and 3, respectively.

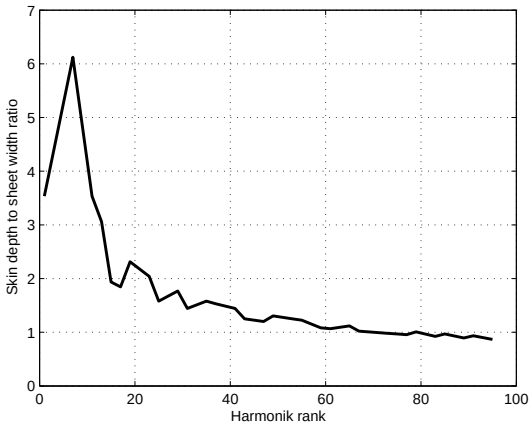


Fig. 2. (Skin depth/ sheet width) vs. harmonic rank in rotor core

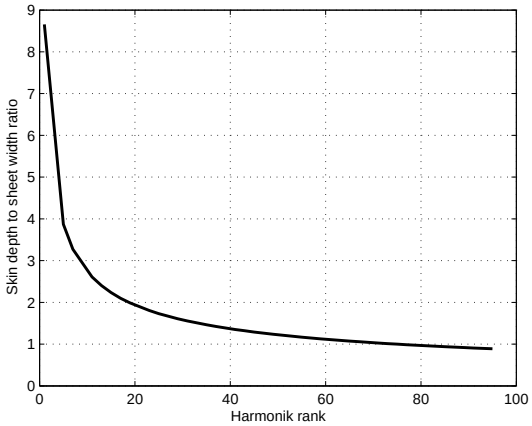


Fig. 3. (Skin depth/ sheet width) vs. harmonic rank in stator core

Taking into account the maximum flux value $\hat{\phi} = \hat{B}al$ and the sheet volume $V = abl$, the expressions of the eddy-current loss per unit volume turn to be at low and high frequencies, respectively:

$$\begin{cases} P_{el} = \dfrac{\omega^2\hat{B}^2a^2\sigma}{24} \\ \\ P_{eh} = \dfrac{\omega^2\hat{B}^2a\delta\sigma}{8} \end{cases} \tag{4}$$

The expressions given by equation (4) are derived in the case of a sinusoidal shape of the flux density. That is to say that the computation of eddy-current losses requires just the peak value of the flux density. However, in the case of FSPMM, the shape of the air gap flux density is far from being sinusoidal either under no-load operation or with the contribution of the armature current.
Taking into consideration the contribution of all harmonics, the computation of eddy-current losses is then formulated at low and high frequencies, respectively:

$$\begin{cases} P_{el} = \sum_{k=1}^{\infty} \dfrac{\omega_k^2\hat{B_k}^2a^2\sigma}{24} \\ \\ P_{eh} = \sum_{k=1}^{\infty} \dfrac{\omega_k^2\hat{B_k}^2a\delta_k\sigma}{8} \end{cases} \tag{5}$$

where:

$$\begin{cases} \omega_k : & \text{the relative angular speed of k}^{\text{th}} \text{ rank} \\ \hat{B_k} : & \text{the flux density peak value of k}^{\text{th}} \text{ rank} \\ \delta_k : & \text{the skin depth of k}^{\text{th}} \text{ rank} \end{cases}$$

## 3. Derivation of the Flux Density Waveform Produced by the PMs

Figure 4 illustrates the air gap flux density distribution versus the mechanical angle created by the PMs , whose *Fourier* transform is expressed as follows [10]:

$$\begin{cases} B_{pm}(r) = \sum_{n=1,3,5..}^{\infty} K_{bn}F_r(r)\cos(np_r\theta) \\ \\ B_{pm}(\theta) = \sum_{n=1,3,5..}^{\infty} K_{bn}F_\theta(r)\sin(np_r\theta) \end{cases} \tag{6}$$

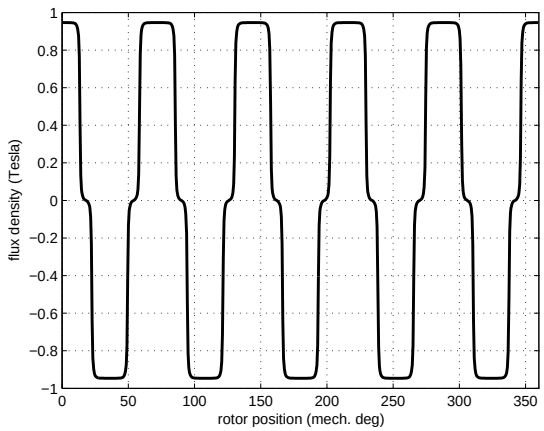


Fig. 4. Spatial repartition of the PM flux density

where:

$$K_{bn} = \frac{4B_r}{\pi\mu_r}\ \frac{p_r}{((np_r)^2-1)}\ \sin\left(\frac{n\pi\beta_{pm}}{2}\right)\left\{\frac{(np_r-1)+2\left(\frac{R_{or}}{R_m}\right)^{(np_r+1)}-(np_r+1)\left(\frac{R_{or}}{R_m}\right)^{2np_r}}{\left(\frac{\mu_r+1}{\mu_r}\right)\left(1-\left(\frac{R_{or}}{R_{is}}\right)^{2np_r}\right)-\left(\frac{\mu_r-1}{\mu_r}\right)\left(\left(\frac{R_m}{R_{is}}\right)^{2np_r}-\left(\frac{R_{or}}{R_m}\right)^{2np_r}\right)}\right\} \quad (7)$$

and where:

$$\begin{cases} F_r(r)=\left(\frac{r}{R_{is}}\right)^{(np_r-1)}\left(\frac{R_m}{R_{is}}\right)^{(np_r+1)}+\left(\frac{R_m}{r}\right)^{(np_r+1)} \\ F_\theta(r)=\left(\frac{R_m}{r}\right)^{(np_r+1)}-\left(\frac{r}{R_{is}}\right)^{(np_r-1)}\left(\frac{R_m}{R_{is}}\right)^{(np_r+1)} \end{cases} \quad (8)$$

with:

$$R_m = \begin{cases} R_{is} & - & \delta \\ R_{or} & + & h_{pm} \end{cases} \quad (9)$$

where:

- $p_r$ is the rotor pole pair number,
- $R_{is}$ is the radius at the stator surface,
- $R_m$ is the radius at the magnet surface,
- $R_{or}$ is the radius at the rotor core surface,
- $B_r$ is the magnetic remanence of the PMs,
- $\beta_{pm} = \frac{w_{pm}}{\tau_{pr}}$ is the magnet width to pole pitch ratio.

The analysis of the PM flux density is then achieved by the representation of its harmonic spectrum which is illustrated in figure 5.

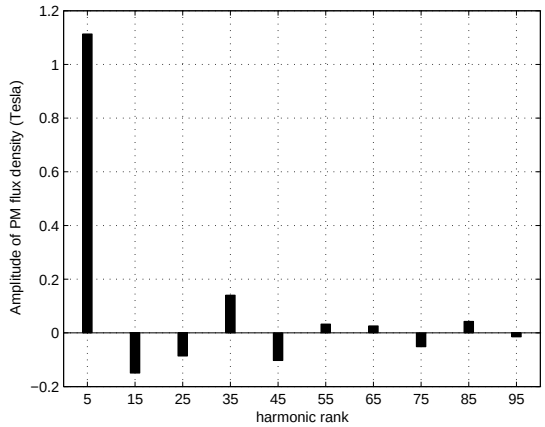


Fig. 5. Spectrum of the air gap flux density created by PMs

Each harmonic of rank $k$ is characterized by an amplitude $B_k$, and an angular frequency $\omega_k$. The sign of the contribution of each harmonic affects the calculation of the harmonic speed and then the eddy-current loss.
In the case of positive sign, the harmonic rotates in the same direction as the synchronous one. On the contrary, a negative sign is characterized by a rotation of the harmonic of rank $k$ and the synchronous one in opposite directions.

## 4. Derivation of the Flux Density Produced by the Armature

Let us consider the case where the concentrated winding PM machine is fed by sinusoidal currents, with:

$$\begin{cases} i_a &= \hat{I}\cos(\omega t) \\ i_b &= \hat{I}\cos(\omega t-\frac{2\pi}{3}) \\ i_c &= \hat{I}\cos(\omega t+\frac{2\pi}{3}) \end{cases} \quad (10)$$

Referring to [4], one can write the *Fourier* transform of the magnetomotive force (M.M.F) generated by phase "a" as follows:

$$\mathcal{F}_{an} = \frac{N}{2\pi}\frac{\sin(n\ \beta\ \frac{\pi}{2})}{n}\Big\{\cos(n\theta)-\cos(n(\theta-\tfrac{\pi}{6})) - \cos(n(\theta-\pi))+\cos(n(\theta-\tfrac{7\pi}{6}))\Big\}\hat{I}\cos(\omega t) \quad (11)$$

The development of equation (11) leads to the following expression:

$$\mathcal{F}_{an}(\theta) = C\sin(n(\theta-\frac{\pi}{12}))\cos(\omega t) \quad (12)$$

where:

$$C = -\frac{N\hat{I}}{\pi}\sin(\frac{n\beta\pi}{12})\sin(\frac{n\pi}{12})(1+(-1)^{n+1})$$

Similarly, M.M.Fs generated by phases "b" and "c" can be deduced from the one of phase "a" as follows:

$$\begin{cases} \mathcal{F}_{bn}= C\sin(n(\theta-\frac{\pi}{12}-\frac{2\pi}{3}))\cos(\omega t-\frac{2\pi}{3}) \\ \mathcal{F}_{cn}= C\sin(n(\theta-\frac{\pi}{12}+\frac{2\pi}{3}))\cos(\omega t+\frac{2\pi}{3}) \end{cases} \quad (13)$$

The superposition of $\mathcal{F}_{an}$, $\mathcal{F}_{bn}$ and $\mathcal{F}_{cn}$ given by equations (12) and (13) leads to the following expression:

$$\mathcal{F}_n = -\frac{N\hat{I}}{\pi}\sin(\frac{n\beta\pi}{12})\sin(\frac{n\pi}{12})(1+(-1)^{n+1}) \Big[\sin(n(\theta-\frac{\pi}{12})-\omega t)(1+2\cos\left(\frac{2\pi(n+1)}{3}\right) + \sin(n(\theta-\frac{\pi}{12})+\omega t)(1+2\cos\left(\frac{2\pi(1-n)}{3}\right)\Big] \quad (14)$$

Finally, the general expression of the M.M.F derived for each harmonic is given in the following:

$$\mathcal{F}_n = \begin{cases} 3C\sin(n(\theta-\frac{\pi}{12})+\omega t) \text{ for n} = 1,4,7... \\ 3C\sin(n(\theta-\frac{\pi}{12})-\omega t) \text{ for n} = 2,5,8... \\ 0 \text{ for n multiple of } 3 \end{cases} \quad (15)$$

Therefore, and giving the relation between the flux density and the M.M.F, such that:

$$B_a(\theta) = \frac{\mu_0}{\delta'}\ \mathcal{F}_n(\theta) \tag{16}$$

where $\delta'$ is the effective air gap width, one can deduce the spatial repartition of the air gap flux density produced by the armature, as shown in figure 6.

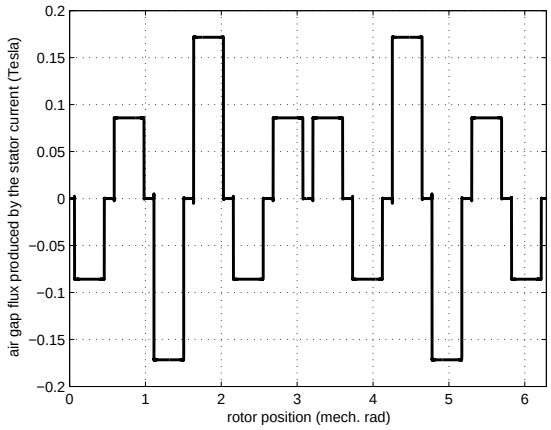


Fig. 6. Flux density produced by the armature under sinusoidal current supply

Accounting for equation (16), one can represent the spectrum of the armature flux density $B_a$ as illustrated in figure 7.

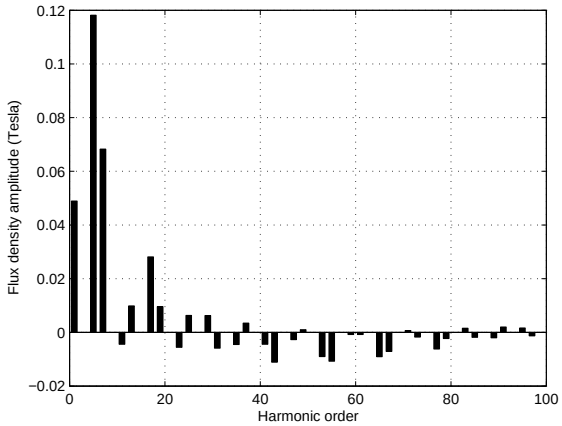


Fig. 7. Armature flux density spectrum

Referring to figures 5 and 7, it is to be noted that beyond the fundamental of rank five, the main contributor to the developed torque, there are multiple harmonics that do not produce torque, and consequently, lead to an increase of the eddy-current losses.

## 5. Analysis of the Resultant Flux Density

Assuming an infinite permeability for the stator and rotor magnetic circuits, the analysis is reduced to a linear problem. As a result, the instantaneous field distribution under any specified load condition can be obtained by the superposition of the open-circuit and armature reaction field components [10]. Under such assumption, the resultant flux density $B_l$ is expressed as:

$$B_l = B_{pm} + B_a \tag{17}$$

A special attention should be paid in the selection of the angular shift between the two phasors $B_{pm}$ and $B_a$ in order to achieve a maximum average torque. In the case of the double-layer topology, such a shift is equal to $\frac{7\pi}{12}$. The resultant flux density $B_l$ is shown in figure 8.

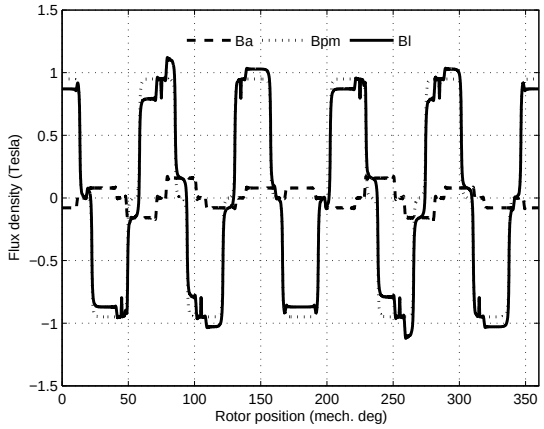


Fig. 8. Resultant air gap flux density $B_l$

The spectrum resulting from the superposition of the armature flux density $B_a$ and the PM one $B_{pm}$ is illustrated in figure 9.

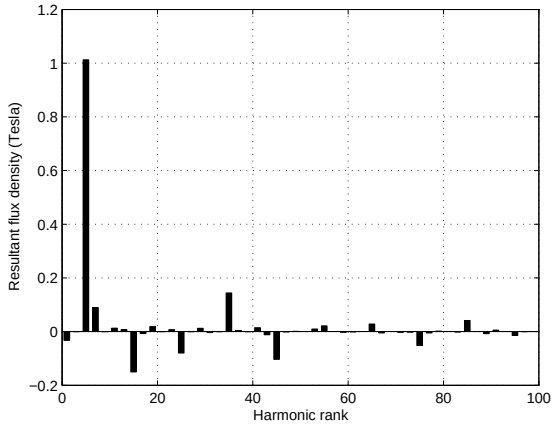


Fig. 9. Resultant flux density spectrum

Referring to figure 9, one can clearly notice that such a spectrum is full of super harmonics. It also includes one sub harmonic of rank one.

## 6. HARMONIC SPEED CALCULATION

The M.M.F harmonics rotate in the air-gap at different speeds, whose expressions $\omega_{rk}$ and $\omega_{sk}$ with respect to the rotor and the stator, respectively, are:

$$\begin{cases} \omega_{rk} &= 2\pi f_s(sig - \frac{k}{p_r}) \\ \omega_{sk} &= 2\pi f_s \frac{k}{p_r} \end{cases} \quad (18)$$

where the function $sig = 1$ when the harmonic and the rotor rotate in the same direction, and $sig = -1$ when the harmonic and the rotor rotate in opposite directions.

## 7. CASE STUDY

### A. Machine Layout

The studied machine has double-layer slots filled by concentrated windings as shown in figure 10. Its major geometrical parameters are listed in table I.

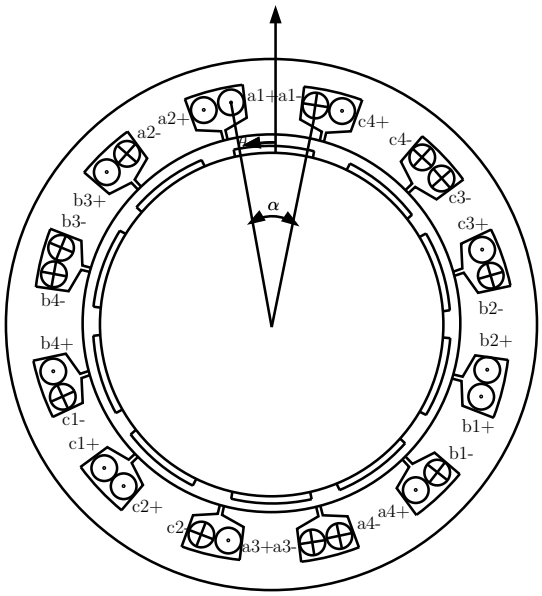


Fig. 10. View of the CWPMM under study

TABLE I
SELECTED CWPMM PARAMETERS

| | |
|---|---|
| number of phases $q$ | 3 |
| number of slots $N_s$ | 12 |
| number of poles $p_r$ | 10 |
| ( coil pitch)/(pole pitch) $\beta$ | 0.125 |
| (magnet width)/(pole pitch) $\beta_{pm}$ | 0.75 |
| rotor outer radius $R_{or}$ | 66mm |
| stator outer radius $R_{os}$ | 117mm |
| air gap $\delta$ | 0.5mm |
| permanent magnet height $h_{pm}$ | 4mm |

### B. Eddy-Current Losses Results

In the calculation of eddy-current losses, it is assumed that:

- the relative magnetic permeability of the iron is $\mu_{rfe} = 200$
- the resistivity of the iron is $\rho_{fe} = 0.25\mu\Omega m$

Figures 11, 12, and 13 show eddy-current losses per volume unit, induced by each harmonic of the flux densities of the PMs, the armature, and their resultant, respectively, in the stator lamination core.

Figures 14, 15, and 16 illustrate eddy-current losses per volume unit, induced by each harmonic of the flux densities of the PMs, the armature, and their resultant, respectively, in the stator lamination core.

Table II gives the predicted eddy-current losses considering the developed formulation applied to the studied machine.

TABLE II
EDDY-CURRENT LOSSES ASSESSMENT

| | No-load | Armature | Load |
|---|---|---|---|
| Rotor losses | 17.79 | 0.38W | 16.32W |
| Stator losses | 52.15W | 1.25W | 49.86W |

Referring to the results illustrated in figures 11 to 16 and to the data given in table II, three major remarks could be distinguished:

- considering just the eddy-currents caused by the synchronous harmonic leads to very underestimated losses. For higher ranks, an increase of the eddy-current losses is noticed even with the decrease of the harmonic amplitude. Such an increase of the losses is due to the increase of the harmonic speed.
- the losses at no-load operation are more important than those induced by the armature supposed acting separately. This is due to the important amplitude of the no-load flux density reaching 1.01T for the fundamental compared to the armature one which does not exceed 0.12T.
- even though the studied machine is a synchronous type one with a laminated rotor, the eddy-current losses in the latter are not negligible as in machines with sinusoidally-distributed armature winding. In the studied machine, the eddy-current losses in the rotor are almost third of the stator ones.

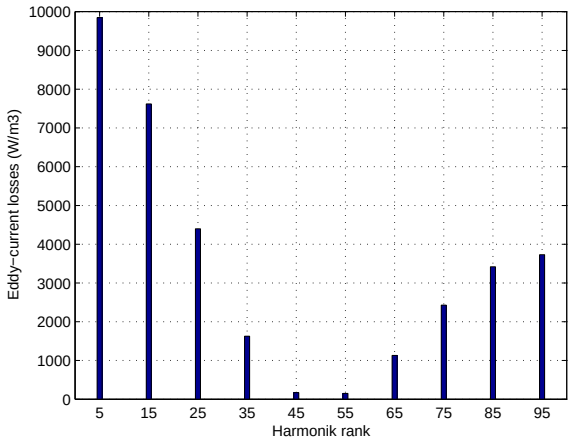


Fig. 11. No-load eddy-current losses in the stator yoke

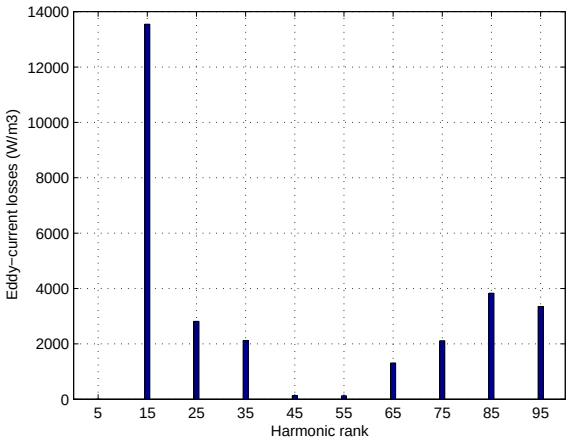


Fig. 14. No-load eddy-current losses in the rotor yoke

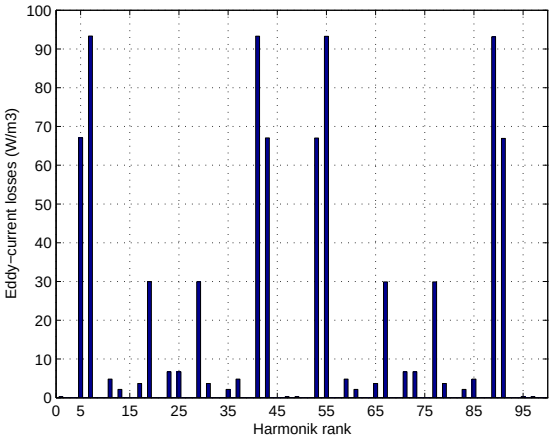


Fig. 12. Armature eddy-current losses in the stator yoke

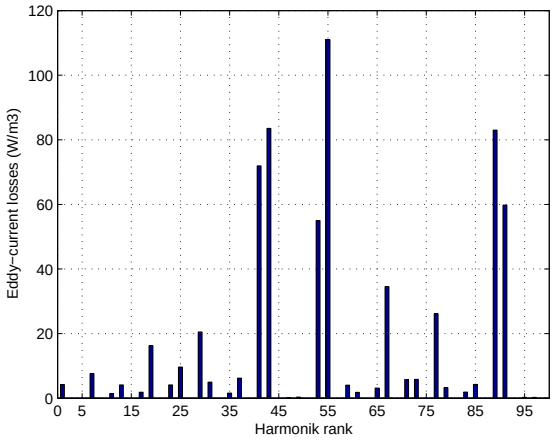


Fig. 15. Armature eddy-current losses in the rotor yoke

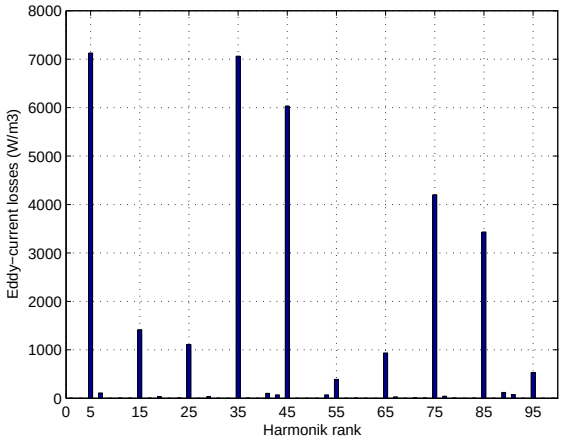


Fig. 13. Eddy-current losses in the stator yoke resulting from PMs and armature contributions

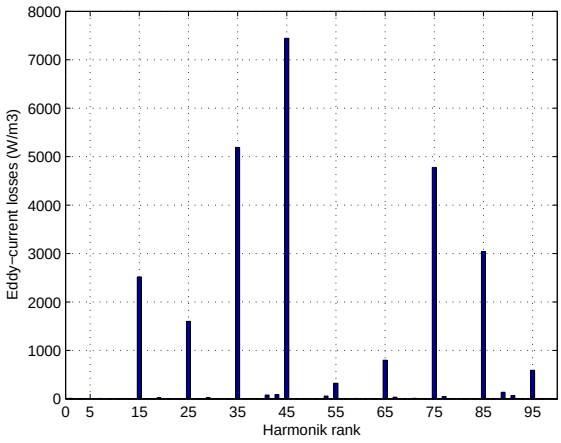


Fig. 16. Eddy-current losses in the rotor yoke resulting from PMs and armature contributions

## 8. CONCLUSION

The paper was aimed at a prediction of eddy-current losses in concentrated winding machines. The prediction had been based on splitting the air gap flux density waveform into its harmonics. The analysis has been carried out considering the flux density produced by permanent magnets as well as the one of the armature. Moreover, the skin depth effect has been taken into consideration in the formulation of eddy-current losses. It has been found that considering just the eddy-currents caused by the fundamental harmonic leads to very underestimated losses. For higher ranks, an increase of the eddy-current losses is noticed even with the decrease of the harmonic amplitude. Furthermore, even with a laminated rotor, the eddy-current losses in the latter are not negligible as in synchronous machines with sinusoidally-distributed armature winding.

## REFERENCES


[1] N. Bianchi, M. Dai Pre, L. Alberti and E. Fornasiero, "Theory and design of fractional-slot PM machines," Tutorial course notes, *Industry Applications Society Annual Meeting*, New Orleans, USA, September 2007.

[2] A. M. El-Refaie, T. M. Jahns, P. J. McCleer and J. W. McKeever, "Experimental verification of optimal flux weakening in surface PM machines using concentrated windings," *IEEE Transactions on Industry Applications*, vol. 21, no. 2, pp. 362-369, 2006.

[3] D. Ishak, Z. Q. Zhu and D. Howe "Eddy-current loss in the rotor magnets of permanent-magnet brushless machines having a fractional number of slots per pole,"*IEEE Trans. on Magnetics*,vol. 41, no. 9, pp. 2462-2469, 2005.

[4] G. Ben Hamadou, A. Masmoudi, I. Abdennadher and A. Masmoudi, "Design of a single-stator dual-rotor permanent magnet machine application to electrical propulsion systems," *IEEE Trans. on Industry Applications*, vol. 45, no. 1, pp. 1-6, 2009.

[5] C. C. Mi, G. R. Slemon, R. Bornert, "Modeling of iron losses of permanent-magnet synchronous motors", *IEEE Trans. Industry Applications*, vol. 39, no. 3, pp. 734-742, 2003.

[6] Y. Chen, P. Pillay, "An improved formula for lamination core loss calculations in machines operating with high frequency and high flux density excitation," *IEEE 37th IAS Annual Meeting*, vol. 2, pp. 759-766, October 2002.

[7] H. Polinder, M. J. Hoeijmakers and M. Scuotto,"Eddy-current losses in the solid back-iron of permanent magnet machines with concentrated fractional pitch windings," *in proc. 2006 IEE International Conference on Power Electronics, Machines and Drives*, Dublin, pp. 479-483, April 2006.

[8] N. Bianchi and E. Fornasiero, "Impact of MMF space harmonic on rotor losses in fractional-slot permanent-magnet machines,"*IEEE Trans. Energy Conversion*, vol. 24, no. 2, pp. 323-328, 2009.

[9] J. Barranger,"Hysteresis and eddy-current losses of a transformer lamination viewed as an application of the poyting theorem,"*NASA technical note* D-3114, pp 10-12, 1965.

[10] Z. Q. Zhu, D. Ishak, D. Howe, and J. Chen, "Unbalanced magnetic forces in permanent-magnet brushless machines with diametrically asymmetric phase windings,"*IEEE Trans. Industry Application*,vol. 43, no. 6, pp. 1544-1553, 2007.